Catalysis Science & Technology

PAPER

View Article Online
View Journal

Cite this: DOI: 10.1039/c5cy01675d

Influencing the activity and selectivity of alkylaromatic catalytic transformations by varying the degree of delamination in MWW zeolites

Mogahid Osman,[a] Sulaiman Al-Khattaf,*[a] Urbano Díaz,[b] Cristina Martínez[b] and Avelino Corma*[b]

Received 1st October 2015,
Accepted 25th November 2015

DOI: 10.1039/c5cy01675d

www.rsc.org/catalysis

The degree of delamination and chemical composition of MWW zeolites have been varied by adjusting the synthesis parameters and modifying the temperature of the swelling step applied to the layered precursor (MCM-22(P)), and their impact on the catalytic behavior of these MWW materials for alkylaromatic transformation reactions has been studied. Kinetic experiments performed in a fluidized-type riser simulator have allowed us to establish a complete reaction network and to discern the impact of the catalyst's variables on competing alkylation and transalkylation of alkylbenzene molecules. In this way, the positive effect of delamination of the MWW layered precursor regarding the selectivity for the alkylation product with respect to transalkylation and catalyst deactivation has been confirmed by comparing a microporous MCM-22 with a highly delaminated ITQ-2 obtained from the same layered precursor, and also for 3D MCM-22 and highly delaminated ITQ-2 with comparable acidic properties.

1. Introduction

Aromatic alkylation is an important catalytic process that leads to the production of high value alkylaromatics such as ethyltoluene, ethylbenzene and xylenes.[1,2] Thus, ethylbenzene is commonly used as a raw material for the manufacture of styrene[3,4] and *p*-ethyltoluene is used as a monomer in the production of poly-*p*-methylstyrene, an alternative to polystyrene due to its superior properties.[3] On the other hand, aromatic alkylation reactions are also used as model reactions for the characterization of zeolite structures, as the activity and selectivity results obtained can be correlated with the pore dimensions, presence of cavities and acidic properties of the zeolites studied.[5–14]

HCl, HF, solid H_3PO_4 and Friedel–Crafts alkylation catalysts like $AlCl_3$, are involved in many problems regarding their handling, safety, corrosion and waste disposal and have been substituted by zeolite-based catalysts, which offer clear environmental improvements and thermal and hydrothermal stability while giving high activity and product selectivity.[15–17] Zeolites are microporous crystalline materials that have been extensively used as sorbents and catalysts in petroleum refining, petrochemical processes, and, more recently, in the production of fine chemicals and pharmaceuticals.[15] Among the different zeolites known,[18] MCM-22 (IZA structure code MWW) has aroused great interest due to its peculiar pore structure and acidic properties. Its structure was solved by Leonowicz *et al.*[19] and has been commercially applied for the liquid phase alkylation of benzene with ethene and propene to ethylbenzene and cumene, respectively.[20] Zeolite MCM-22 is obtained by calcination of the layered precursor MCM-22(P), which causes the topotactic condensation of the MWW layers. Its structure presents two independent pore systems, the first one formed by ten-membered-ring (10MR) sinusoidal pores running within the layers, and the second one formed by intralayer twelve-membered ring (12MR) supercages (7.1 × 7.1 × 18.2 Å) connected by double six-membered ring (6MR) units, and its synthesis and characterization have been thoroughly described in the literature.[7,19,21,22] The influence of the special structural features of MCM-22 on its catalytic behavior was already shown for different model reactions such as *m*-xylene isomerization/disproportionation and *n*-decane hydroisomerization.[7] Besides its microporous structure, zeolite MCM-22 presents a high proportion of external Brønsted acid sites, accessible through the semi-cavities formed on the external surface.[19,21] The double porosity of MCM-22 has also an important influence on its stability towards deactivation: the large supercages can trap molecules, which undergo many successive reactions leading to deposits of carbonaceous compounds (coke), while the sinusoidal channel system seems less affected by deactivation.[23,24] A wide variety of catalytic applications of MCM-22 has been reported, such as

[a] *Center of Research Excellence in Petroleum Refining & Petrochemicals, King Fahd University of Petroleum & Minerals, 31261 Dhahran, Saudi Arabia. E-mail: skhattaf@kfupm.edu.sa; Fax: +966 3 860 4509; Tel: +966 3 860 2029*
[b] *Instituto de Tecnología Química (UPV-CSIC), Universidad Politécnica de Valencia, Consejo Superior de Investigaciones Científicas, Valencia, 46022, Spain. E-mail: acorma@itq.upv.es; Fax: +34 963879444; Tel: +34 963877800*

alkylation,[25–30] isomerization,[5,23,24,31–33] disproportionation,[7,22,34–37] cracking,[38–41] methanol-to-olefin conversion,[42] aromatization of methane[43–45] and other reactions.[31,46,47]

An interesting aspect of zeolite MCM-22 is that its layered precursor can be swollen, exfoliated and pillared under suitable conditions, allowing different arrangements of the MCM-22 monolayers.[48,49] Moreover, the delaminated zeolite ITQ-2 was successfully synthesized by exfoliating and dispersing the layers by means of ultrasonic treatment or, in a more industrial way, by fast stirring of the suspension.[50] ITQ-2 is formed by exfoliated crystalline sheets of 2.5 nm thickness,[38,50–52] and the monolayers present open 12R hemicavities at the external surface. Thus, the high accessibility of its active sites improves the activity and the catalyst life of ITQ-2 as compared to microporous MCM-22 when used in reactions involving bulky molecules such as conversion of bulky alkylbenzenes and catalytic cracking of vacuum gas oil.[26,52–56] ITQ-2 has been investigated for 1,3,5-tri-isopropylbenzene dealkylation and cumene cracking and showed excellent results in accommodating the large molecules.[57] Cracking of light cycle oil (LCO) also had been studied using ITQ-2 as a catalyst and the performance was found to be comparable with that of large pore zeolites, such as USY and Beta.[39] Higher propylene selectivity and better stability was achieved during dehydrogenation of propane over ITQ-2 supported gallium oxide due to the higher accessibility, minor diffusion problems, and lower amount of strong Brønsted acid sites of the ITQ-2 catalyst.[58]

Delamination of MCM-22(P) to ITQ-2, besides increasing the accessibility of the active Brønsted acid sites, also has a direct effect on the acid site density and acid strength.[59] It would be very interesting to obtain a suitable correlation between the role of acidity and the degree of delamination. The aim of this work is to identify and correlate the influence of acid site density and level of delamination of MWW-based zeolites on their behavior when used as catalysts in the competing alkylation and transalkylation reactions occurring during alkylation of toluene by alcohols or olefins.

Therefore, ITQ-2 with different degrees of delamination and MCM-22 with different Si/Al ratios, and therefore with different number of Brønsted acid sites, were synthesized and used for catalyzing various reactions, *e.g.* toluene ethylation, benzene ethylation, toluene disproportionation and ethylbenzene methylation. A suitable kinetic model has been developed for the reactions studied based on an extensive set of kinetic experiments performed in a fluidized-bed reactor. The kinetic parameters have been used to explain the role of acidity and level of delamination for directing into the different products.

2. Experimental methods

2.1. Materials

2.1.1 Synthesis of MWW lamellar zeolitic precursors (MCM-22(P)) with different Si/Al ratios. MCM-22(P) zeolitic precursors with MWW-type structure and different aluminum content (Si/Al = 25–80), based on inorganic layers connected together by a layer of organic structural directing agents (hexamethyleneimine, HMI), were prepared through hydrothermal synthesis. Typically, 0.365 g of sodium aluminate (56% Al_2O_3, 37% Na_2O, Carlo Erba) and 0.375 g of sodium hydroxide (98%, Prolabo) were dissolved in 80.71 g of distilled water, after which 4.96 g of HMI (98%, Aldrich) and 6.00 g of silica (Aerosil 200, Degussa) were added consecutively. This mixture was stirred vigorously for 30 minutes at room temperature, producing a gel with a silicon-to-aluminum atomic ratio of 25 (corresponding silica-to-alumina molar ratio of 50). The crystallization of the lamellar precursor was done at 423 K for 9 days under dynamic conditions in a PTFE-lined stainless-steel autoclave (35 cc volume) tumbled at 40 rpm under autogenous pressure. The crystalline product was filtered and washed with distilled water until pH $<$ 9. The MWW material was filtered and dried at 333 K for 12 hours.

Through a similar methodology, several MCM-22(P) lamellar precursors were obtained with different Si/Al molar ratios following the synthesis conditions shown in Table 1.

2.1.2 Synthesis of delaminated ITQ-2 materials starting from MCM-22(P) with Si/Al = 25. In order to prepare each of the layered ITQ-2 zeolites, 10 g of the lamellar MWW precursor (MCM-22(P)) with Si/Al = 25 were dispersed in 40 g of Milli-Q H_2O, and 200 g of a cetyltrimethylammonium hydroxide solution (25 wt%, 50% exchanged Br/OH) and 60 g of a solution of tetrapropylammonium hydroxide (40 wt%, 30% exchanged Br/OH) were added until a pH $\geq$12.5 was reached. The resultant mixture was heated at different temperatures (323 K for ITQ-2-A, 338 K for ITQ-2-B and 353 K for ITQ-2-C) and vigorously stirred for 16 hours in order to facilitate the swelling of the precursor material's layers. At this point, the suspension was sonicated in an ultrasound bath (50 W, 50 Hz) for 1 hour to disperse the individual sheets. Then, the pH was decreased to 3.0 by adding drop by drop a 6 M HCl solution in order to facilitate the flocculation of the delaminated solid, which was then recovered by centrifugation and washed with distilled water. After drying at 333 K for 12 hours, the solid was calcined for 3 hours at 813 K in N_2 and then for 6 hours in air (2.5 ml s^{-1} flow, heating rate of 3° min^{-1}). With this calcination treatment all the organic compounds were decomposed, yielding a material having the structural and textural characteristics of ITQ-2.

2.1.3 Synthesis of MCM-22 zeolites with different Si/Al ratios. MCM-22 zeolites with different Si/Al ratios were obtained by calcination of the as-synthesized MCM-22(P) samples in air for 3 hours at 853 K. In this way the 3D microporous structure was formed by topotactic condensation of the individual zeolitic MWW layers after elimination of the structure-directing compounds located in the interlayer space. The samples were named MCM-22(25) and MCM-22(80).

2.2. Catalyst characterization

Powder X-ray diffraction (PXRD) patterns of the calcined samples were recorded on a Philips X'Pert diffractometer equipped with a graphite monochromator, operating at 40 kV and 45 mA, and using nickel-filtered CuKα radiation (λ = 0.1542 nm).

Table 1 Experimental conditions to prepare MWW lamellar precursors (MCM-22(P)) with different aluminum contents (gel composition, time and temperature of the hydrothermal syntheses)

Sample	Si/Al	SiO_2/Al_2O_3	OH/SiO_2	Na/SiO_2	HMI/SiO_2	H_2O/SiO_2	T (K)	t (days)
MCM-22(25)	25	50	0.10	0.14	0.35	45	423	9
MCM-22(80)[a]	80	160	0.11	0.18	0.50	45	408	8

[a] Seeding with MCM-22 (Si/Al = 25), 35 wt% in relation to total SiO_2.

The chemical composition of the catalysts was analyzed in a 715-ES ICP-optical emission spectrometer after dissolution of the solids in a HNO_3/HCl/HF solution.

Textural properties were determined from the nitrogen adsorption isotherm measured at 77 K on a Micrometrics ASAP 2010 volumetric adsorption analyzer. Surface area and micropore volume values were obtained by applying the BET equation and from the *t*-plot graph, respectively.

Acidity measurements were carried out by adsorption/desorption of pyridine followed by IR spectroscopy. Self-supported wafers (10 mg cm^{-2}) of calcined samples, previously activated at 673 K and 10^{-2} Pa overnight in a Pyrex vacuum cell, were allowed to come in contact with 6.5×10^2 Pa of pyridine vapor at room temperature and desorbed in vacuum at increasing temperatures (423, 523, and 623 K). The spectra were recorded at room temperature. All the spectra were scaled according to the sample weight. Adsorption coefficients calculated by Emeis[60] were used. Analogous experiments but using 2,6-di-*tert*-butylpyridine (DTBPy)[61] as probe molecule were also carried out to measure the external acidity.

2.3. Alkylation reactions in a fluidized CREC Riser Simulator

Alkylation reactions of toluene, ethylbenzene and benzene with alcohols were conducted in a fluidized CREC Riser Simulator which is a bench scale equipment with an internal recycle unit.[62] The reactor details and the experimental procedure can be found elsewhere.[63]

All experiments were conducted using 0.80 g of catalysts with particle size of 60 μm and a mass of reactant injected of 0.162 g, residence times of 5, 10, 15 and 20 seconds, temperatures of 473, 498, 523, 573 and 623 K, and atmospheric pressure. The particle size of 60 mm, adequate for fluidization under the conditions of the CREC Riser Simulator, was obtained by grounding and sieving of catalyst pellets. All runs were fed with equimolar mixtures of aromatics and alcohols. The riser simulator was heated under a continuous flow of argon (inert gas). The catalyst was thermally activated at 893 K for 15 minutes in a stream of air. After each run the product gas samples were analyzed three times by automatic injection into the gas chromatograph (GC). The standard deviations at each run were found to be in the range of ±2%. The GC analyzed data were further processed to calculate the conversion, product yield and selectivity.

2.4. Kinetic modelling

Kinetic models demonstrating the alkylation rate are developed based on Scheme 1 and the observed data obtained from the fluidized-bed reactor. Isothermal operating conditions were assumed given the design of the riser simulator and the relatively small amount of reacting species. Under the studied experiment conditions the alkylation reactions were considered to be free from internal and external mass transfer limitations. The internal diffusion can also be considered to be negligible for the studied reaction kinetic using ITQ-2 and MCM-22 as catalysts. Similar kinetic studies by Marin and co-workers demonstrated a negligible diffusion effect on the reaction kinetics for ethylbenzene dealkylation over Pt promoted HZSM-5 zeolite.[64]

The rate of reaction for each reacting species for toluene ethylation and ethylbenzene methylation can be written as follows:

• Toluene alkylation with ethanol:

Rate of reaction for toluene

$$-\frac{V}{W_c}\frac{dC_T}{dt} = \left(k_1 C_T C_{EtOH} + 2k_2 C_T^2\right)\exp(-\alpha t) \quad (1)$$

Rate of reaction for ethyltoluene

$$\frac{V}{W_c}\frac{dC_{EtTol}}{dt} = \left(k_1 C_T C_{EtOH}\right)\exp(-\alpha t) \quad (2)$$

Rate of reaction for xylene

$$\frac{V}{W_c}\frac{dC_{Xy}}{dt} = \left(k_2 C_T^2\right)\exp(-\alpha t) \quad (3)$$

Rate of reaction for benzene

$$\frac{V}{W_c}\frac{dC_{Bz}}{dt} = \left(k_2 C_T^2\right)\exp(-\alpha t) \quad (4)$$

Rate of reaction for gases

$$\frac{V}{W_c}\frac{dC_G}{dt} = \left(k_3 C_{EtOH}\right)\exp(-\alpha t) \quad (5)$$

• Ethylbenzene alkylation with methanol:

Rate of reaction for ethylbenzene

$$-\frac{V}{W_c}\frac{dC_{EB}}{dt} = \left(k_1 C_{EB} C_{MtOH} + 2k_2 C_{EB}^2\right)\exp(-\alpha t) \quad (6)$$

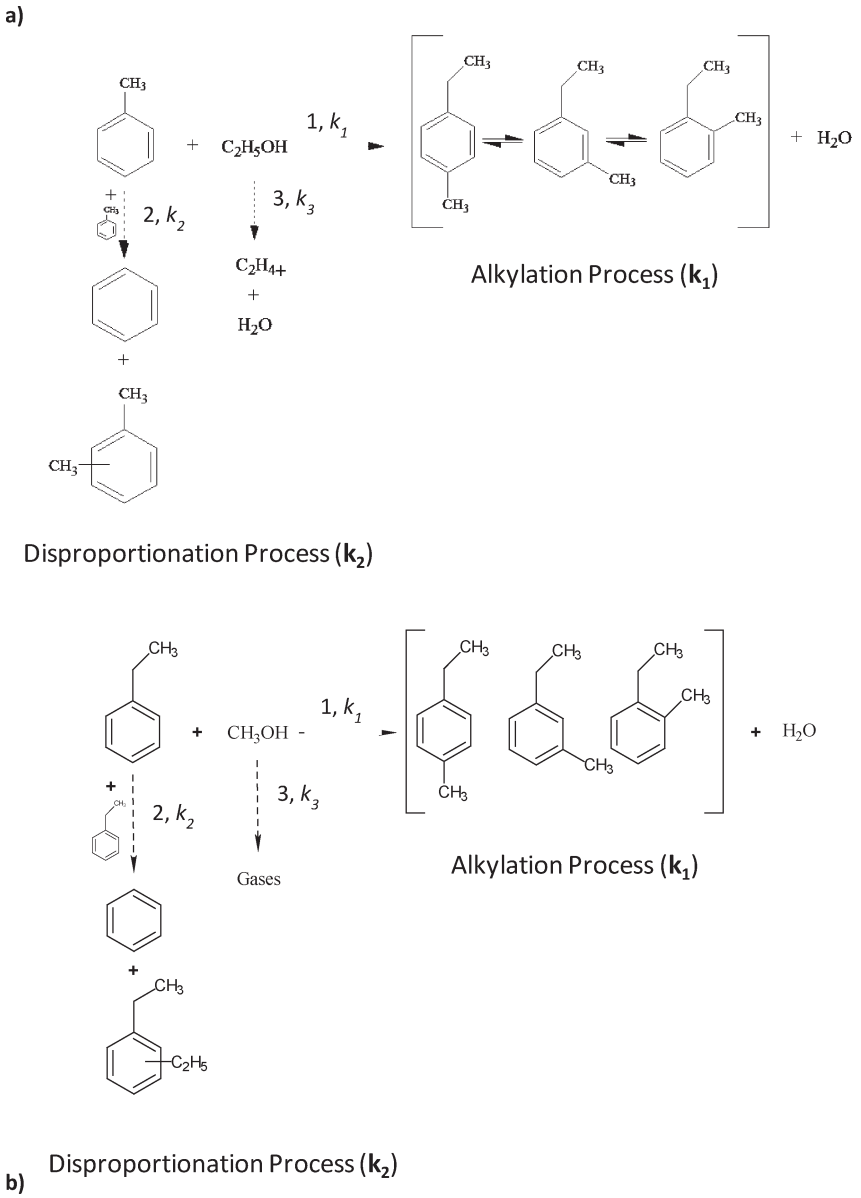

Scheme 1 Reaction paths for (a) toluene alkylation with ethanol and (b) ethylbenzene alkylation with methanol.

Rate of reaction for ethyltoluene

$$\frac{V}{W_c}\frac{dC_{EtTol}}{dt} = \left(k_1 C_{EB} C_{MtOH}\right)\exp\left(-\alpha t\right) \quad (7)$$

Rate of reaction for diethylbenzene

$$\frac{V}{W_c}\frac{dC_{DEB}}{dt} = \left(k_2 C_{EB}^{\ 2}\right)\exp\left(-\alpha t\right) \quad (8)$$

Rate of reaction for benzene

$$\frac{V}{W_c}\frac{dC_{Bz}}{dt} = \left(k_2 C_{EB}^{\ 2}\right)\exp\left(-\alpha t\right) \quad (9)$$

Rate of reaction for gases

$$\frac{V}{W_c}\frac{dC_G}{dt} = \left(k_3 C_{MtOH}\right)\exp\left(-\alpha t\right) \quad (10)$$

where C_i is the molar concentration of each species in the system, V is the volume of the reactor, W_c is the mass of the catalyst, t is the time in seconds, k_i is the rate constant of each species, and α is the catalyst deactivation constant.

The molar concentration C_i can be expressed in terms of the weight fraction of each species y_i, which are the measurable variables from the chromatographic analysis; hence,

$$C_i = \frac{y_i W_{hc}}{MW_i V} \quad (11)$$

where W_{hc} is the weight of feedstock injected into the reactor and MW_i is the molecular weight of the species.

The rate constant was represented with the temperature dependence form of the Arrhenius equation given as:

$$k_i = k_{i0} \exp\left[-\frac{E_i}{R}\left(\frac{1}{T} - \frac{1}{T_0}\right)\right] \quad (12)$$

where k_{i0} and E_i are the pre-exponential factor and activation energy of the reaction i, respectively. T_0 is referred to as the centering temperature which is the average of all the temperatures for the experiment in order to reduce parameter interaction.

The mole balance equations incorporating the Arrhenius relation were evaluated by a least squares fitting of the kinetic parameters using the experimental data obtained for the toluene ethylation reaction. The MATLAB ODE 45 (4th-order Runge–Kutta method) subroutine was used for solving the differential equation, while the lsqcurvefit function was employed for the least squares fitting of the kinetic parameters. The kinetic model was selected according to the following criteria: (i) all the kinetics parameters (specific reaction rates and activation energies) should be consistent with physical principles, (ii) coefficient of determination (R^2), (iii) lower SSR (sum of the squares of the residuals), (iv) lower cross-correlation coefficient (γ), and (v) smaller individual confidence intervals for the model parameters.

3. Results and discussion

3.1. Catalyst characterization

Increasing delamination of the MWW laminar precursor results in increased accessibility to the active sites and therefore in higher efficiency for catalyzing processes dealing with bulky molecules.[59] However, partial loss of Brønsted acid site density and acid strength has been described to occur during the different steps of the delamination procedure. Thus, the objective of this work is to study the influence of both the degree of delamination – different levels of accessibility – of ITQ-2 samples with comparable Al content, and the effect of the Si/Al ratio on 3D MCM-22 samples, which will present different amounts of Brønsted acid sites, but no delamination. As detailed in the experimental section, the different delamination levels were obtained by using different swelling temperatures (323 K, 338 K and 353 K for samples ITQ-2-A, ITQ-2-B and ITQ-2-C, respectively) during the preparation route.

The powder XRD patterns corresponding to the calcined MCM-22 and the three ITQ-2 samples are shown in Fig. 1. The 6–10° 2θ range (Cu Kα radiation) of the XRD patterns gives valuable information regarding the layers' arrangement and the interlayer interactions of MWW materials. So, the loss of order of the individual MWW layers along the "c" axis in the delaminated ITQ-2 zeolites is evidenced by the absence of the two (001) and (002) bands in the 3–7° 2θ range. Moreover, the patterns of these samples show broad diffraction bands as compared to the MCM-22 zeolite due to the strong crystal size

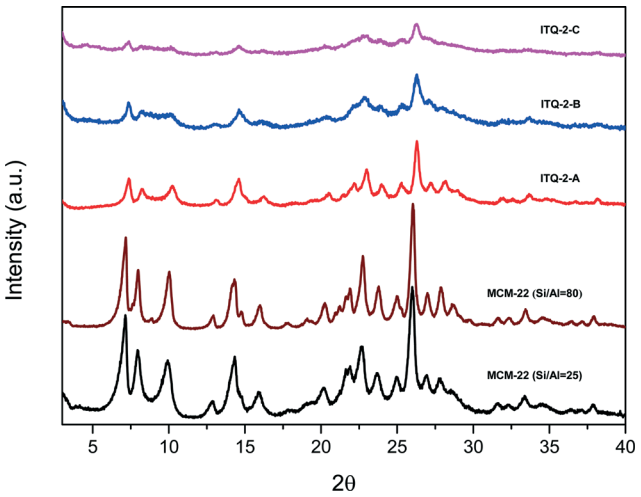

Fig. 1 XRD patterns.

reduction combined with the long order loss as a consequence of the delamination process. Finally, it has to be remarked that, although less intense, the diffraction bands ($hk0$) representative of the *ab* planes of each individual MWW layer are observed for the ITQ-2 materials, indicating a significant preservation of the zeolitic sheets during the exfoliation step. Comparing the ITQ-2 zeolites, a decrease in the intensity of the diffraction bands was observed when increasing the swelling temperature from ITQ-2-A to ITQ-2-C, indicating a progressive increase of the degree of delamination from A to C.

The nitrogen adsorption isotherms obtained for the four calcined zeolites are compared in Fig. 2. MCM-22 presents an isotherm close to a type I, representative of microporous materials. The isotherm corresponding to ITQ-2-A, obtained by swelling the laminar precursor at the lowest temperature, presents a very similar shape, indicating that this material is only slightly delaminated. As the severity of the delamination procedure increases, the shape of the isotherm gets closer to that of a type IV, typical of disordered mesoporous materials. The textural properties calculated from these N_2 isotherms

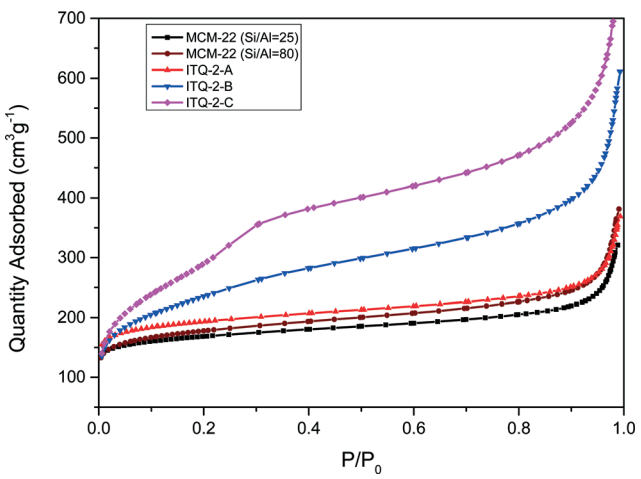

Fig. 2 N_2 adsorption isotherms.

are enclosed in Table 2. Indeed, the higher the swelling temperature during the delamination procedure, the higher the BET surface, mainly due to an increase in the external surface of the samples. On the other hand, the micropore volume of the most delaminated ITQ-2-C is significantly reduced as compared to that of the 3D MCM-22. Thus, the degree of delamination has been varied between a purely microporous MCM-22 and a highly delaminated zeolite with around 750 $m^2\ g^{-1}$ of external surface and reduced micropore volume (0.019 $cm^3\ g^{-1}$).

Although the different ITQ-2 materials were prepared starting from the same MCM-22(P) sample with a gel Si/Al ratio of 25, the chemical composition presented in Table 2 evidences an increasing dealumination of the zeolites obtained by swelling at higher temperatures. Still, the Si/Al ratios of all the samples are maintained within the range of 25–35.

The micropore volume loss and the slight dealumination observed when increasing the degree of delamination from ITQ-2-A to ITQ-2-C will have a direct effect on the number of Brønsted acid sites of the acid zeolites. Indeed, Table 3 shows how the Brønsted acid site density as measured by pyridine adsorption–desorption decreases in the order MCM-22 > ITQ-2-A > ITQ-2-B > ITQ-2-C. It has to be noted that not only the total number of acid sites but also the amount of pyridine retained at different desorption temperatures changes when increasing the degree of delamination, with a lower proportion of the sites able to retain pyridine at 623 K remaining on the most delaminated material. The degree of delamination also has a clear effect on the amount of accessible Brønsted acid sites, closer to the external surface of the zeolites as can be deduced from the results enclosed in the last column of Table 3. There it can be seen that the proportion of sites able to protonate the bulky 2,6-di-*tert*-butylpyridine (DTBPy) is below 10% for the non-delaminated MCM-22 and increases gradually from samples ITQ-2-A to ITQ-2-C as the external surface area increases. In fact, all the acid sites determined for ITQ-2-C, the most delaminated MWW, are accessible to DTBPy. Regarding the Lewis acidity, the total amount of sites and the proportion of strong Lewis sites do not vary significantly when comparing MCM-22(25) and delaminated ITQ-2-A and ITQ-2-B. However, higher severity of the delamination conditions results in a lower amount of strong Lewis sites (see sample ITQ-2-C).

With the aim of decoupling the influence of acidic and textural properties of MWW materials on the toluene alkylation/disproportionation reaction, an additional MCM-22 sample with a lower Al content has been synthesized, MCM-22(80), with Si/Al ratio in the gel of 80. Its physico-chemical properties are included in Table 2. It can be seen that the Al content of the final solid is in good agreement with that in the synthesis gel and that both MCM-22 zeolites present comparable textural properties. However, the reduction of the Al content has a direct effect on the total Brønsted acid site density (see Table 3) given by the amount of sites that are able to retain pyridine at 423 K. It also has an effect on the amount and proportion of the sites with stronger acid strength, which retain the basic probe at a desorption temperature of 623 K. In fact, comparing the acidity results obtained for all the MWW samples, it can be seen that zeolite MCM-22(80) has acidic properties comparable to those of ITQ2-C, the sample with the largest degree of delamination, in terms of number of sites and strength distribution. Still, there is an important difference regarding the accessibility of these sites, as only 8% of the Brønsted sites are external sites in the case of MCM-22(80), whereas all the sites are external in the case of ITQ2-C. Finally, and as could be expected, the MCM-22(80) sample, synthesized with a higher Si/Al ratio, presents a lower amount of Lewis acid sites, probably because it is more stable towards framework dealumination. By comparing the catalytic behavior of these samples it will then be possible to determine the contribution of delamination at a comparable acidity level.

3.2. Catalytic tests on aromatic alkylation with light alcohols

As mentioned in the experimental section, the catalytic alkylation of toluene with ethanol and of ethylbenzene with methanol was carried out in a fluidized riser simulator over

Table 2 Comparison of the physico-chemical properties of the MWW samples

Sample	Si/Al	S_{BET} ($m^2\ g^{-1}$)	S_{micro} ($m^2\ g^{-1}$)	S_{Ext} ($m^2\ g^{-1}$)	V_{Tot} ($cm^3\ g^{-1}$)	V_{micro} ($cm^3\ g^{-1}$)	V_{BJH} ($cm^3\ g^{-1}$)
MCM-22(25)	25	426	347	79	0.505	0.168	0.147
MCM-22(80)	76	454	355	99	0.520	0.170	0.155
ITQ2-A	27	586	267	319	0.589	0.106	0.298
ITQ2-B	30	729	115	614	0.690	0.059	0.534
ITQ2-C	35	828	74	754	0.817	0.019	0.723

Table 3 Comparison of the acidic properties of the MWW samples

	Brønsted				Lewis			
Sample	423 K	523 K	623 K	B623/B423	423 K	523 K	623 K	% External sites (DTBPy)
MCM-22(25)	64	56	48	0.75	24	22	20	7
MCM-22(80)	24	18	10	0.42	14	12	9	8
ITQ2-A	57	39	29	0.51	26	22	20	24
ITQ2-B	35	27	14	0.40	22	21	20	61
ITQ2-C	21	15	9	0.41	23	20	15	100

different MCM-22 and ITQ-2 catalysts, with the aim of investigating the effect of the MWW degree of delamination and acidity on the performance of the different reactions involved in the process. Alkylation of aromatics with alcohols catalyzed by acidic zeolites is considered as an electrophilic substitution on the aromatic ring and proceeds through a carbonium ion-type mechanism.[65] The alcohol is dehydrated in a first step, forming water and a surface alkyl cation which can follow two different pathways, as shown in Scheme 1, for toluene ethylation (a) and ethylbenzene methylation (b): the cationic intermediate can further react with the aromatic to produce the desired alkylation product after releasing the proton to the surface (reaction 1), or it can oligomerize to longer chain intermediates which can be transformed into other secondary products through cracking, isomerization and alkylation (reaction 3). On the other hand, alkylaromatics, such as toluene, can also undergo disproportionation reactions, yielding benzene and xylenes (see reaction 2 in Scheme 1a). These disproportionation reactions were shown to proceed involving bimolecular intermediates, in which the aromatic rings are bridged by a carbon atom of the alkyl group.[66] The structure of the zeolite (pore sizes and topology), its Brønsted acid site density and the reactivity of the alkylation agents used are known to have an important influence on the extension of the competing disproportionation reaction.[8,13,33,67–70] Previous results have shown that toluene disproportionation is favored when the structure of the zeolite used as catalyst presents cavities, such as in TNU-9 or MCM-22.[13,33,68–70] Thus, the amount of cages present in the MCM-22 zeolites and remaining in the partially delaminated ITQ-2 samples compared in this work, which is directly related to their degree of delamination, is expected to have a direct influence on the contribution of the different reactions and, therefore, on the product distribution obtained. Thus, it could be predicted that from the textural characteristics point of view, alkylation will be favored on the more delaminated MWW zeolites, whereas toluene disproportionation will take place to a larger extent when carrying out the reaction in the presence of 3D MCM-22 or with the less delaminated ITQ-2-A.

3.2.1 Toluene alkylation with ethanol. The activity of the catalysts has been compared at 523 and 573 K in Fig. 3a and b, respectively. Conversion was varied by increasing the residence time in the range of 5–20 seconds. Although the differences among the compared samples become smaller with increasing temperature, the most active catalyst is the purely microporous MCM-22 in both cases, and the aromatic conversion obtained decreases when the degree of delamination of the ITQ-2 zeolites is increased. According to these results, and in a first approximation, it could be concluded that the toluene conversion is mainly influenced by the acidity of the catalyst and that the increasing accessibility gained by delamination has no positive effect. At this point it is important to bear in mind that the conversions obtained in this reaction system are cumulative values and will therefore be affected by the deactivation rate of the different catalysts. Moreover, the level of delamination and, consequently, the ratio of external to internal surface area, are expected to have an impact on the deactivation of the catalyst. Thus, an additional sample, MCM-22(80), has been included in the plots. This 3D MCM-22 zeolite has a Brønsted acid site density and acid strength distribution close to those of the highly delaminated sample ITQ-2-C. This high degree of delamination results in an increased accessibility of the Brønsted acid sites, as discussed in the former section. Comparison of the catalytic results obtained with these two MWW materials, presenting similar acidity but different accessibility to these sites, should give information regarding the effect of delamination. The plots presented in Fig. 3 show that toluene conversion obtained with the microporous MCM-22(80) is lower than that of the delaminated ITQ-2C, despite the slightly higher overall acidity of the former. Comparing the conversion curves obtained for these two samples it can be concluded that under the conditions studied here and for MWW samples of similar acidity, delamination has a positive effect from the point of view of toluene conversion. The higher accessibility of the active sites and the reduced diffusion path lengths result in a decreased extension of undesired reactions, such as polyalkylations, which may lead to coke precursors and are known to deactivate the catalyst with time on stream during toluene ethylation.[8]

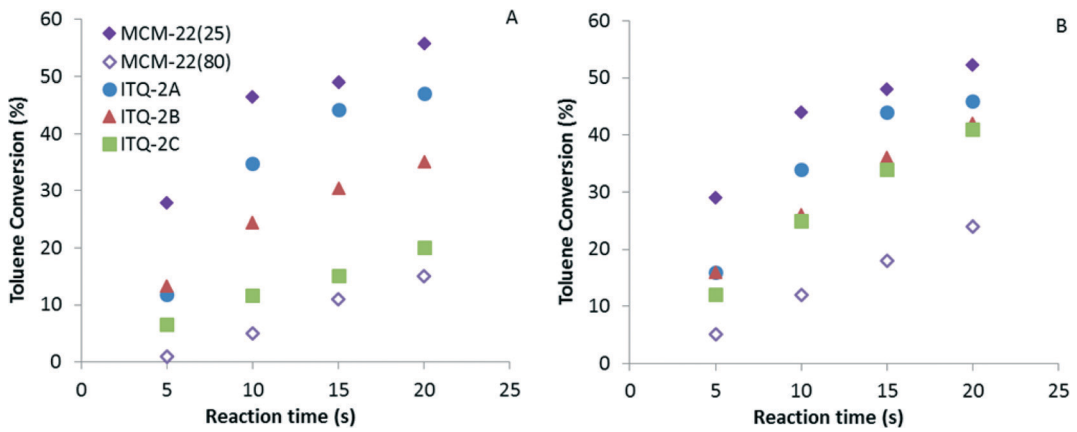

Fig. 3 Toluene alkylation with ethanol: toluene conversion at different residence times. (A) T = 523 K, (B) T = 573 K.

On the other hand, and taking into account the reaction scheme presented in Fig. 3, toluene can be converted not only by alkylation with the alcohol (reaction 1) but also through disproportionation reactions to benzene and xylenes (reaction 2), and the density of Brønsted acid sites should have an impact on the relative rate of these two reactions.[3] Moreover, toluene disproportionation has been shown to be favored in zeolites presenting cavities in their structures such as MCM-22 or TNU-9.[13,33,68–70] Therefore, the activity for toluene disproportionation on this 3D zeolite will be especially sensitive to the decrease in the active site density.

Table 4 details the conversion and yields to the different products obtained at 523 K and at the different residence times for the two MCM-22 zeolites with different Si/Al content and for the three ITQ-2 samples. In all cases, ethyltoluene (ET) obtained by means of reaction 1 (Scheme 1) is the main product obtained. Benzene and xylenes are also present in the product mixture in a significant proportion, indicating that toluene disproportionation (reaction 2 in Scheme 1) is contributing to the overall conversion, and benzene alkylation products, such as ethylbenzene (EB) and diethylbenzene (DEB) are also observed. Fig. 4 shows the selectivity plots corresponding to the main products. Comparing MCM-22(25) with the different ITQ-2 samples shows a clear correlation of the selectivity for ET with the degree of delamination of the zeolites. In fact, 3D MCM-22(25) is the less selective for this primary alkylation product and, as we increase the degree of delamination, the selectivity for ET increases. As in the case of toluene conversion, this could be explained by the decreasing acidity of the more delaminated samples because toluene disproportionation proceeds through a bimolecular pathway and will, therefore, be favored by a high density of Brønsted acid sites.[71] On

Table 4 Conversion and product distribution for different reaction times (T = 523 K)

Catalyst	Time	Toluene conv.%	Ethanol conv.%	Gases	Benzene	EB	Xylene	*p*-EtTol	*m*-EtTol	*o*-EtTol	EtTol	DEB	Other
MCM-22(25)	20	55.76	76.50	5.48	2.61	8.15	10.64	8.16	15.19	3.31	26.67	4.91	2.78
	15	48.97	70.69	6.14	2.31	7.44	9.20	8.83	13.89	3.03	25.75	2.42	1.85
	10	46.40	51.65	4.11	2.46	7.07	8.35	7.91	12.45	2.72	23.07	3.75	1.70
	5	27.94	31.82	3.61	1.66	4.57	4.59	4.94	7.75	1.71	14.40	1.85	0.86
MCM-22(80)	20	14.94	43.07	6.33	0.37	1.77	1.57	5.64	3.54	1.08	10.27	0.97	0.90
	15	11.26	28.00	5.51	0.23	1.17	1.00	4.68	2.57	0.92	8.15	0.71	0.85
	10	4.92	19.53	4.07	0.14	0.56	0.44	1.73	1.39	0.50	3.62	0.16	0.80
	5	0.56	13.00	3.64	0.00	0.00	0.00	0.12	0.28	0.16	0.56	0.00	0.31
ITQ-2-A	20	47.05	74.48	4.71	1.90	6.40	8.75	6.93	13.48	2.96	23.37	6.62	2.33
	15	44.17	68.56	4.69	1.68	5.67	7.73	7.10	12.91	2.84	22.85	6.23	2.18
	10	34.79	48.25	3.84	1.27	4.54	5.59	6.16	10.39	2.28	18.84	4.56	2.03
	5	11.80	22.76	2.37	0.46	1.60	1.53	2.66	3.64	0.87	7.16	1.05	1.08
ITQ-2-B	20	35.14	67.39	5.12	0.59	2.58	3.18	7.78	13.12	3.36	24.25	4.54	2.78
	15	30.35	58.96	5.75	0.49	2.05	2.53	7.34	11.13	3.04	21.50	3.78	1.85
	10	24.44	46.59	5.04	0.42	1.79	2.37	5.89	8.77	2.35	17.01	2.84	1.70
	5	13.25	27.20	3.02	0.32	1.22	1.27	3.32	4.70	1.19	9.20	1.24	0.86
ITQ-2-C	20	20.04	57.48	8.38	0.16	0.72	0.80	6.18	6.68	3.29	16.15	2.21	1.60
	15	15.14	42.97	8.02	0.13	0.55	0.56	5.32	4.42	2.63	12.37	1.52	1.23
	10	11.71	33.72	5.98	0.15	0.50	0.44	4.37	3.28	1.99	9.63	0.98	1.14
	5	6.55	16.63	3.36	0.10	0.40	0.33	2.47	1.95	0.90	5.32	0.40	0.70

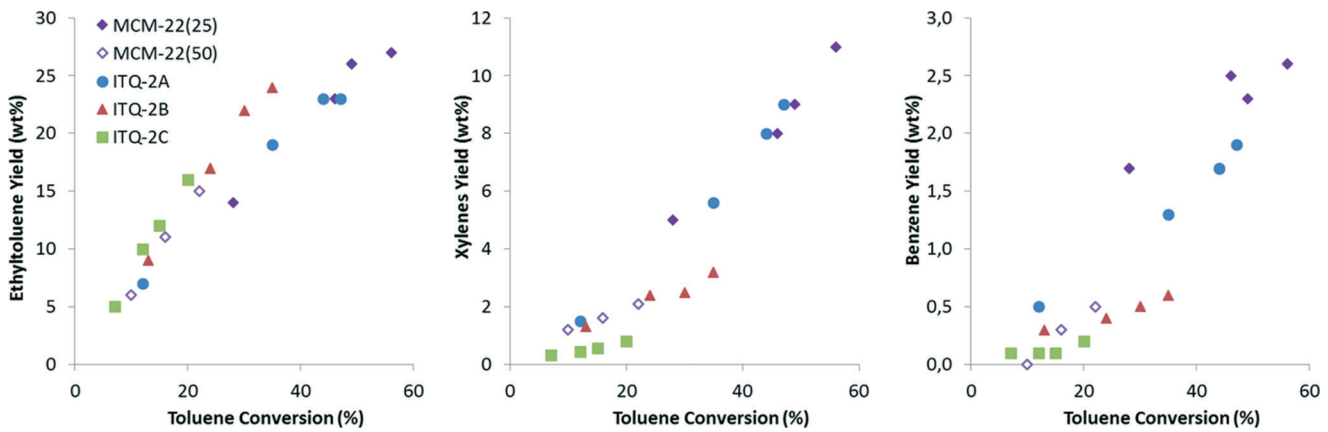

Fig. 4 Toluene alkylation with ethanol: selectivity for the main products. T = 523 K.

the other hand, it could also be due to the increasing degree of delamination, which will result in a reduction of the amount of cavities remaining, where toluene disproportionation is expected to occur. Comparing the selectivity results obtained with samples ITQ-2-C and the more dealuminated MCM-22(80) with different degrees of delamination but comparable acidity, it can be seen that ITQ-2 is more selective for the alkylation product and yields a lower amount of disproportionation compounds, benzene and xylenes, and of EB and DEB obtained by secondary alkylation of benzene. Thus, comparing the accessibility of the active sites at constant acidity, delamination has a positive effect for enhancing the desired alkylation reaction and reducing the extension of competitive secondary reactions. Regarding the rest of the products observed, gases are also produced, mainly ethene obtained by dehydration of ethanol, part of which does not further react. No direct correlation is observed between the amount of gases produced and the Lewis acidity of the samples compared, although these types of acid sites could be playing a role in the alcohol dehydration reaction. Other products, such as diethylbenzene and trimethylbenzene, are enclosed within the "Other" fraction.

Ethanol conversion obtained at a reaction temperature of 523 K as a function of residence time for the different MWW samples is shown in Fig. 5a. When comparing these values with the corresponding toluene conversions, it can be seen that the former values are higher in all cases (see Table 4), as could be expected because alcohol dehydration is a less demanding reaction. Still, the trend observed when comparing the different catalysts is the same as for conversion of toluene. Activity decreases when increasing the degree of delamination of the materials, but when comparing the highly delaminated ITQ-2-C with the non-delaminated MCM-22(80) of comparable acidity, the latter is considerably less active. As the tests are performed with an equimolar toluene : ethanol mixture, the excess of ethene formed by ethanol dehydration may be present in the gases, or it may be involved in the formation of by-products, such as EB and DEB, or oligomers that may lead to deactivation of the catalyst.

As discussed above and shown in Scheme 1, different reactions are taking place on the catalysts studied in our experimental conditions, and their relative contribution to the overall process is different depending on the acidity of the catalysts and on the degree of delamination when compared at constant acidity of the catalyst. The reaction temperature is also expected to have a different effect on the reactions catalyzed by the different samples. Table 5 encloses the results obtained with MCM-22(25), MCM-22(80) and the three ITQ-2 zeolites at 20 s reaction time and four different temperatures, ranging from 473 to 623 K, and ethanol conversion obtained under these conditions is given in Fig. 5b. According to the results presented in Table 5, toluene conversion increases with temperature up to a certain value. In the case of the most active samples, MCM-22(25) and ITQ-2A, it reaches a maximum value at 523 K and decreases when the reaction temperature is further increased. This maximum is much less pronounced and takes place at higher temperatures when we consider the less active samples, *e.g.* ITQ-2B, ITQ-2C or MCM-22(80). In fact, for the latter the highest toluene conversion is obtained at the highest temperature. This behavior with temperature can be explained if we take into account the deactivation of the catalyst. As discussed earlier, in the type of reactor used for this study the conversions and product distributions are average values obtained during the time the catalyst comes in contact with the reaction mixture. Thus, when a catalyst deactivates fast, the results will be affected by this deactivation, and this effect will be larger for longer residence times. This can be clearly seen in Fig. 6. Indeed, when comparing the results obtained at 20 s (Fig. 6a) with those obtained at 5 s (Fig. 6b) it can be seen that at shorter reaction times toluene conversion increases with reaction temperature for all the catalysts except for the most active MCM-22(25), where a maximum is still observed at temperatures around 573 K, although less pronounced than in the case of the longer residence time. At shorter times the degree of deactivation will be lower, and the overall conversion and selectivity values will be less affected by the loss of activity of the catalyst.

Regarding the product distribution obtained at 20 s residence time and different temperatures, presented in Table 5,

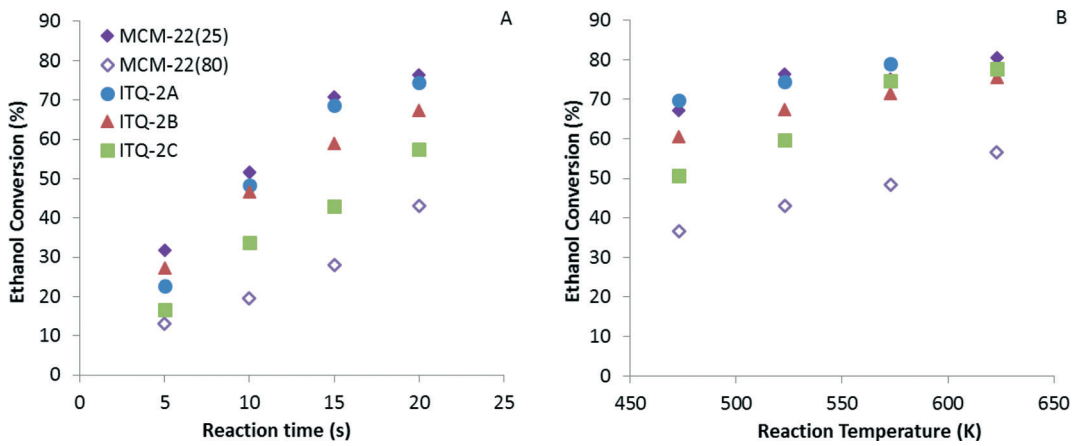

Fig. 5 Toluene alkylation with ethanol: ethanol conversion A) at different residence times and T = 523 K, B) at different temperatures and t = 20 s.

Table 5 Conversion and product distribution for different temperatures (t = 20 s)

Catalysts	T (K)	Toluene conv.%	Ethanol conv.%	Gases	Benzene	EB	Xylene	p-EtTol	m-EtTol	o-EtTol	EtTol	DEB	Other
MCM-22(25)	623	47.16	80.43	12.97	5.67	8.32	15.61	3.40	8.12	2.00	13.52	2.32	1.73
	573	52.19	75.05	9.25	3.86	8.04	14.13	5.26	11.92	2.77	19.95	3.88	2.33
	523	55.76	76.50	5.48	2.61	8.15	10.64	8.16	15.19	3.31	26.67	4.91	2.78
	473	42.63	67.18	2.95	1.36	6.54	6.77	10.98	11.47	2.19	24.64	2.42	0.90
MCM-22(80)	623	23.84	56.52	8.25	1.56	3.03	5.68	3.45	6.79	1.63	11.86	0.00	1.70
	573	24.10	48.44	6.36	0.69	3.12	3.83	5.98	6.97	1.48	14.43	0.00	2.03
	523	14.94	43.07	6.33	0.37	1.77	1.57	5.64	3.54	1.08	10.27	0.00	0.97
	473	4.54	36.63	6.23	0.00	0.21	0.00	3.13	0.00	0.64	4.32	0.00	0.00
ITQ-2A	623	41.98	77.78	10.62	4.83	5.71	12.97	3.53	8.46	2.08	14.07	0.00	4.41
	573	46.17	78.98	8.17	3.22	6.53	11.65	4.93	11.63	2.72	18.35	0.00	6.42
	523	47.05	74.48	4.71	1.90	6.40	8.75	6.93	13.48	2.96	23.37	0.00	6.62
	473	35.63	69.64	3.28	0.90	3.91	4.47	8.85	11.54	2.61	23.00	0.00	3.35
ITQ-2B	623	39.28	75.55	8.68	2.27	4.52	7.98	5.08	11.49	2.91	19.48	0.00	5.03
	573	42.20	71.44	6.10	1.24	3.93	5.90	6.50	14.47	3.50	24.47	0.00	6.65
	523	35.14	67.39	5.12	0.59	2.58	3.18	7.78	13.12	3.36	24.25	0.00	4.54
	473	11.19	60.45	8.81	0.07	0.31	0.23	4.95	2.86	2.38	10.19	0.00	0.38
ITQ-2C	623	39.47	77.71	7.46	1.22	3.13	5.33	6.13	14.23	3.63	23.99	0.00	5.68
	573	40.78	74.71	5.01	0.72	2.70	4.01	7.08	15.35	3.78	26.21	0.00	7.13
	523	20.04	59.68	8.38	0.16	0.72	0.80	6.18	6.68	3.29	16.15	0.00	2.21
	473	6.05	50.66	8.01	0.00	0.00	0.00	2.75	1.23	1.74	5.72	0.00	0.33

the first thing to be noted is that xylenes, coming from the toluene disproportionation reaction, are produced in larger amounts at the highest reaction temperatures. This is especially true for sample MCM-22(25), the microporous zeolite with the highest Brønsted acid site density, where ethyltoluene is not the main product anymore at 623 K, independently of the residence time. From the results enclosed in Table 5 it can also be deduced that despite the higher contribution of toluene disproportionation at increasing temperatures, when the degree of delamination is increased (larger ratio of external to internal surface area and lower amount of Brønsted acid sites) toluene ethylation can be performed with higher selectivity for the primary alkylation product ET. This can be clearly seen in Fig. 7a, where the alkylation/disproportionation ratio (determined as the ratio between the yields to ET and xylenes) is represented for the different MWW materials at increasing temperatures and 20 s reaction time. Comparing the results obtained for the two MCM-22 zeolites, it can be clearly seen that the contribution of the toluene disproportionation reaction is lower in the case of the sample with the highest Si/Al content, and thus, with the lowest acidity, MCM-22(80). It is important to note, however, that although an increase in the Si/Al ratio of the 3D MCM-22 zeolites increases the catalyst's selectivity for the alkylation products, the contribution of the ethylation reaction obtained in the case of the delaminated sample ITQ-2C, with acidity comparable to that of MCM-22(80), is significantly larger than that of any of the MCM-22 samples

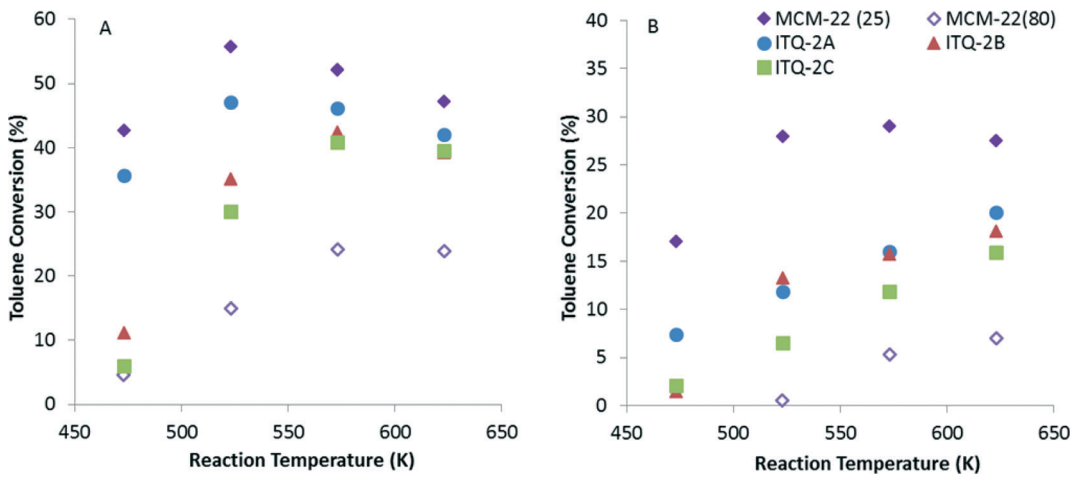

Fig. 6 Toluene alkylation with ethanol: toluene conversion as a function of reaction temperature. (A) TOS = 20 s, (B) TOS = 5 s.

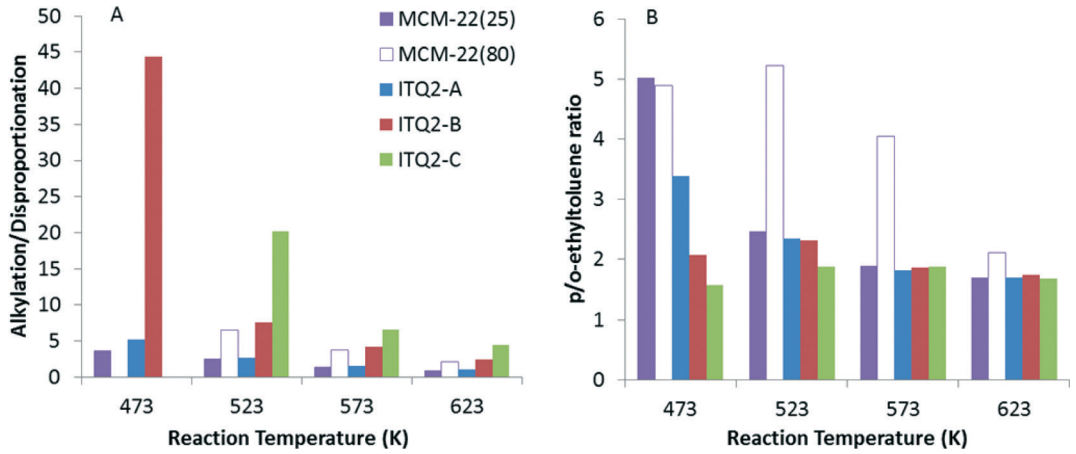

Fig. 7 Toluene alkylation with ethanol: alkylation/disproportionation (A) and *p*/*o*-ethyltoluene (B) ratios as a function of reaction temperature. TOS = 20 s.

compared. The differences in selectivity observed among the catalysts are larger at lower temperatures where kinetic control prevails and, in fact, at 473 K no disproportionation products are observed for the most delaminated ITQ-2-C (results not shown). Thus, the exposure of the active Brønsted sites to the external surface and the drastic reduction of the diffusion path lengths achieved with the delamination of the MCM-22(P) have a predominating role in enhancing toluene alkylation reactions *vs.* toluene disproportionation. Moreover, under those low temperature conditions, the higher contribution of the micropore volume (lower ratio of external to internal surface area) in the case of the non-delaminated MCM-22 and the less delaminated ITQ2-A, is confirmed by the higher *p*-selectivity of these samples, as shown in Fig. 7b.

3.2.2 Benzene alkylation with ethanol and toluene disproportionation. Interesting complementary information regarding the effect of degree of delamination and acidity on the ethylation of toluene can be obtained by studying two closely related additional reactions: benzene alkylation with ethanol, where no disproportionation of the aromatic reactant can take place, and toluene conversion in the absence of any alkylating agent, which will mainly give the toluene disproportionation reaction.

In this section we have limited the comparison to MCM-22(25) and MCM-22(80) and to the most delaminated ITQ-2-C. Conversion curves are obtained by varying the residence time at a constant temperature of 523 K. As was shown for toluene alkylation, the conversion obtained with the delaminated ITQ-2-C during benzene alkylation is slightly lower than the one presented by the microporous MCM-22(25) obtained by calcination of the same layered MWW precursor (see Fig. 8a), and the differences in conversion are less pronounced than in the case of toluene alkylation, where disproportionation of the aromatic was contributing to conversion preferentially on the non-delaminated zeolites.

However, if we compare ITQ-2-C with an MCM-22 zeolite of comparable acidity, MCM-22(80), the delaminated sample is significantly more active for benzene alkylation with ethanol. Regarding the selectivity to the main products, EB and DEB, plotted in Fig. 8b and c, the EB results obtained for the three catalysts fall on the same curve. However, selectivity for DEB is higher for the delaminated ITQ-2-C, in good

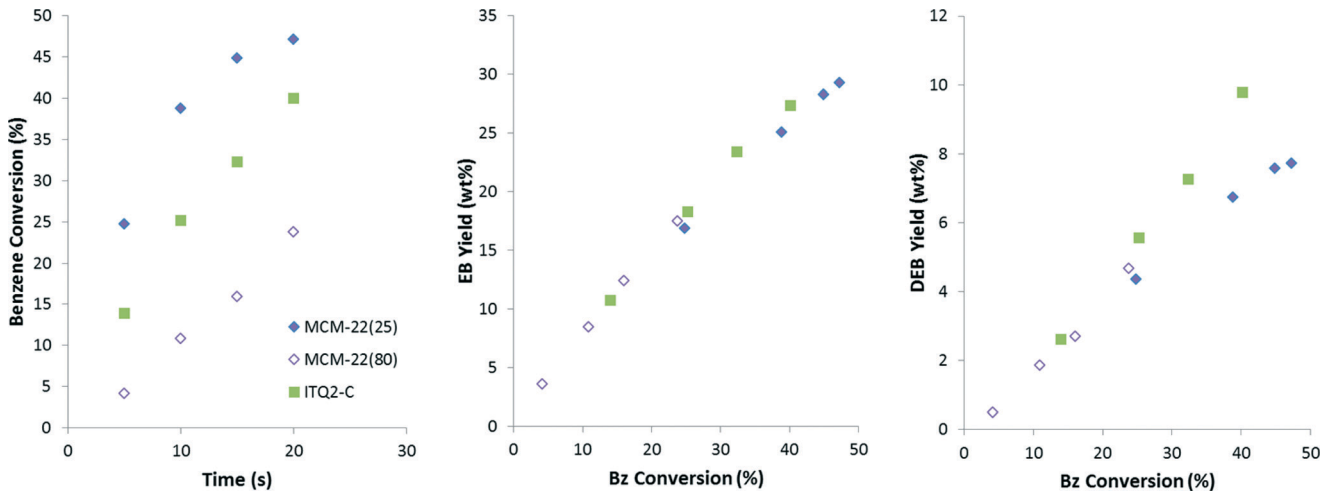

Fig. 8 Benzene alkylation with ethanol: benzene conversion and selectivity for alkylation products at different residence times. *T* = 573 K.

agreement with its higher external surface. The results confirm that, as previously described for alkylation of benzene with light olefins,[25] the alkylation reaction takes place mainly on the external surface of the MWW zeolites, and the role of the microporous structure is negligible regarding benzene alkylation. Thus, for samples with comparable acidity, the higher the amount of accessible sites due to a larger degree of delamination, the higher the activity for aromatic alkylation. The loss of activity due to a reduced acidity observed when comparing MCM-22(25) with MCM-22(80), synthesized with a lower Al content, is compensated for in the case of the ITQ-2 sample by the increased accessibility obtained by means of delamination of the MWW precursor leading to zeolite ITQ2-C.

The same set of catalysts has been used for conversion of toluene by disproportionation at 573 K and different residence times. Toluene conversion and selectivity for the main products, benzene and xylenes, are presented in Fig. 9. In this case there is an important difference regarding the activity of the microporous MCM-22(25) and the other two zeolites compared. Both delamination and acidity loss are in this case highly detrimental to toluene conversion and the values obtained for ITQ-2-C and MCM-22(80) are significantly lower than those obtained in the case of MCM-22(25). Still, the delaminated zeolite is more active than the high silica MCM-22(80), so even for this disproportionation reaction, where the presence of cavities is expected to enhance the conversion of the aromatic, there is a positive effect when a larger external surface is exposed, for samples with comparable Brønsted acid site density. This result can be explained by a reduced catalyst deactivation on the delaminated sample that can result in the higher accumulative conversion observed with ITQ-2-C. No differences are observed regarding selectivity to the main disproportionation products, xylenes and benzene.

3.2.3 Ethylbenzene alkylation with methanol. A different route for obtaining ethyltoluene is by alkylation of ethylbenzene with methanol. Ring alkylation of aromatics with methanol is accepted to proceed *via* chemisorption of methanol on the acid sites. A surface-active species such as a methoxy or methoxonium ion is formed that will further react with the weakly adsorbed aromatic molecule.[72] Moreover, dimethylether (DME) is always present and its contribution to the alkylation process cannot be discarded.

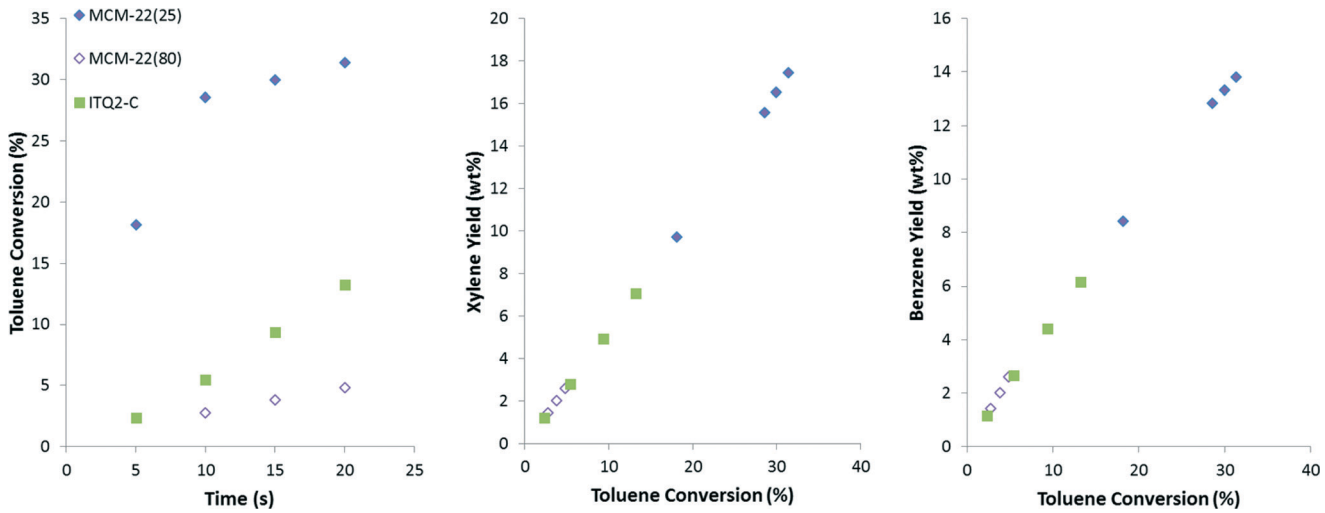

Fig. 9 Toluene disproportionation: conversion and selectivity for main products at different residence times. T = 573 K

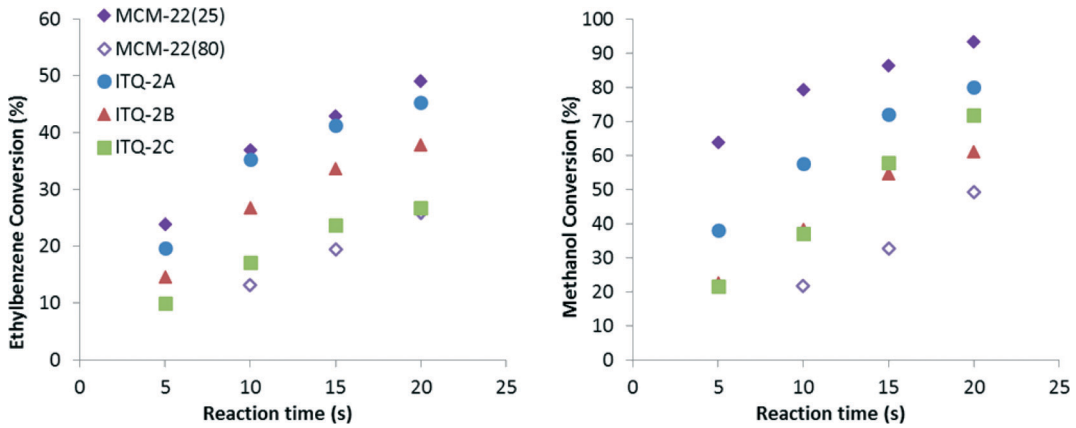

Fig. 10 Ethylbenzene alkylation with methanol: ethylbenzene and methanol conversion at different residence times. T = 573 K.

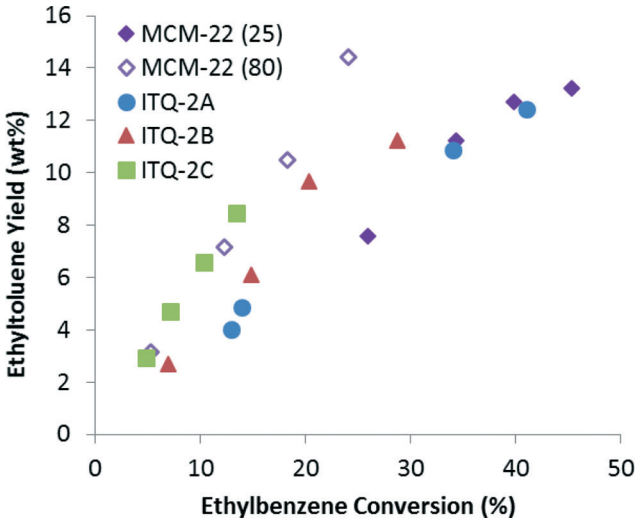

Fig. 11 Ethylbenzene alkylation with methanol: ethyltoluene selectivity curves.

In this case the possible reactions that can take place are those represented in Scheme 1b, on the one hand the alkylation of the aromatic compound (reaction 3), and on the other its competitive disproportionation to benzene and diethylbenzene (reaction 2). However, methanol is more difficult to activate than ethanol, so higher reaction temperatures and/or catalysts with stronger Brønsted acid sites will be required to obtain comparable aromatic conversion levels and ethyltoluene yields. This is indeed the case, as shown in Fig. 10a and b, where the EB and methanol conversion, respectively, are plotted *vs.* reaction time at 573 K. The activity decrease is especially significant when comparing the conversion of the alcohol (see Fig. 5b and 10b) obtained with the most delaminated zeolites ITQ2-B and ITQ2-C, and the high silica MCM-22(80).

Fig. 11 shows the selectivity for ethyltoluene obtained with the different MWW samples at 573 K. The positive effect of the degree of delamination on the selectivity for ET is even more evident when using methanol as alkylation agent. Since methanol is less reactive than ethanol, the catalysts with higher micropore volume and higher Brønsted acid density will convert ethylbenzene to a larger extent by disproportionation reactions and not by alkylation. The most delaminated zeolite ITQ-2-C is now clearly the most selective catalyst for the primary alkylation product.

3.3. Activation energy effect

3.3.1 Toluene alkylation with ethanol. The results obtained for the alkylation of toluene with ethanol at different residence times and temperatures on the MWW zeolites with different degrees of delamination have been adjusted to the kinetic model detailed in section 2.4 and the simplified reaction scheme considered is the one represented in Scheme 1a. Thus, toluene can be converted by alkylation (k_1) or by disproportionation (k_2).

The estimated activation energies obtained from the regression analysis for toluene ethylation and toluene disproportionation are compared in Fig. 12a. According to the results obtained, the activation energy for toluene disproportionation is higher than that of the alkylation reaction and, although the absolute activation energy values increase with the degree of delamination of the MWW zeolite in both cases, this increase is considerably larger for the ethylation reaction. Thus, on non-delaminated or slightly delaminated MWW zeolites alkylation is kinetically favored, but at increasing temperatures the contribution of toluene disproportionation will significantly increase, whereas the temperature effect will be significantly smaller on the highly delaminated ITQ-2-C, and alkylation will predominate within the whole range of temperatures studied.

3.3.2 Ethylbenzene alkylation with methanol. The kinetic study for the methylation of ethylbenzene is based on the simplified reaction scheme presented in Scheme 1b. As in the case of toluene ethylation, the alkylaromatic can react with the alkylation agent or it can suffer disproportionation to benzene and diethylbenzene. Fig. 12b shows that in this case, where methanol is less reactive, the activation energy obtained from the regression analysis is considerably higher for the alkylation reaction than for the disproportionation reaction in the case of the non-delaminated or slightly delaminated materials. When the degree of delamination

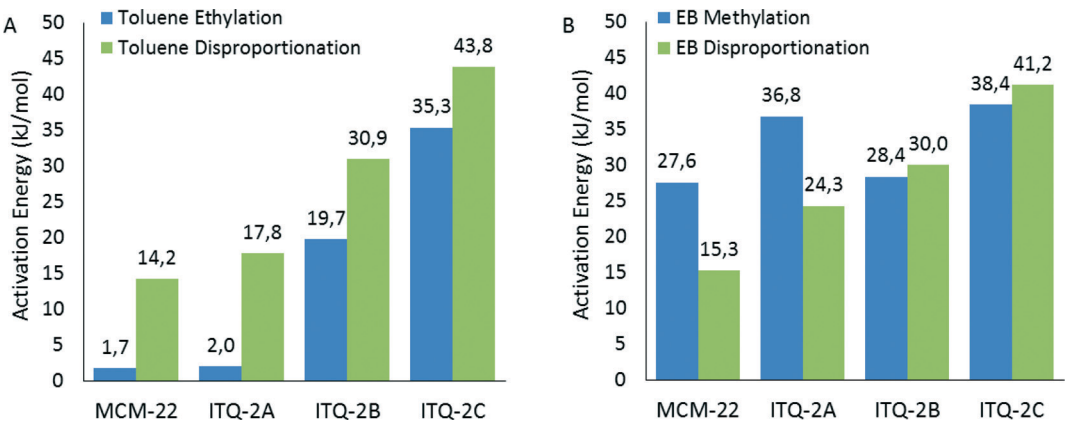

Fig. 12 Activation energies for (A) toluene alkylation with ethanol and (B) EB alkylation with methanol.

increases the activation energy of the two reactions becomes very similar. Thus, disproportionation will be favored when using less reactive alkylation agents, but only when the reaction is catalyzed by non-delaminated MWW zeolites or by ITQ-2 samples with a low degree of delamination.

5. Conclusions

The effect of degree of delamination and Brønsted acid site density has been studied for the alkylation of toluene and ethylbenzene with ethanol and methanol, respectively, and their effect has been decoupled. The aromatic reactants used in these two processes, besides being alkylated, may also be converted by means of disproportionation reactions, and both degree of delamination and amount of active sites are expected to have an important effect on the relative extension of these two competing reactions. The experimental and kinetic study presented here confirms the positive effect of delamination of an MWW layered precursor regarding the selectivity for the alkylation product, as alkylation will be favored *vs.* disproportionation when increasing the degree of delamination, and therefore the ratio of external to internal surface area. This is true not only when comparing the microporous MCM-22 with a highly delaminated ITQ-2 obtained starting from the same layered precursor but also when comparing a 3D MCM-22 and a highly delaminate ITQ-2 presenting comparable acidic properties. In this specific case, ITQ-2 is not only more selective to ethyltoluene but also more active for toluene conversion. Catalyst deactivation is also reduced when increasing the degree of delamination, as evidenced from results obtained by reducing the reaction residence time, and as could be expected due to the higher accessibility and the shorter diffusion path lengths presented by the more delaminated ITQ-2.

When methanol, which is more difficult to activate than ethanol, is used as the alkylation agent, the contribution of the disproportionation reaction increases. However, this effect is much more notorious for the non- or slightly delaminated MWW zeolites. Thus, the benefits of increasing the degree of delamination, especially regarding selectivity to the alkylation products, are even larger than in the case of toluene ethylation.

Notation

C_i Concentration of species i in the riser simulator (mol m^{-3})
CL Confidence limit
E_i Apparent activation energy of the ith reaction (kJ mol^{-1})
k_i Apparent rate constant for the ith reaction (m^3 kg^{-1} of catalysts)
k_{i0} Pre-exponential factor for the ith reaction after re-parameterization (m^3 kg^{-1} of catalysts)
MW_i Molecular weight of species i
r_i Rate of reaction for species i
R Universal gas constant (kJ $kmol^{-1}$ K^{-1})
t Reaction time (s)
T Reaction temperature (K)
T_0 Average temperature of the experiment
V Volume of the riser (45 cm^3)
W_c Mass of the catalyst (0.81 g)
W_{hc} Total mass of the hydrocarbon injected the riser (0.162 g)
y_i Mass fraction of the ith component

Greek letters

α Apparent deactivation function

Acknowledgements

We are grateful for the support from the Ministry of Higher Education, Saudi Arabia, for the establishment of the Center of Research Excellence in Petroleum Refining and Petrochemicals at King Fahd University of Petroleum and Minerals (KFUPM). Financial support by the Spanish Government-MINECO through "Severo Ochoa" (SEV 2012-0267), Consolider Ingenio 2010-Multicat, MAT2012-31657 and MAT2014-52085-C2-1-P, by the European Union by ERC-AdG-2014-671093 (SynCatMatch) and by the Generalitat Valenciana through the Prometeo program (PROMETEOII/2013/011) is acknowledged.

References

1 S. Al-Khattaf, S. A. Ali, A. M. Aitani, N. Žilková, D. Kubička and J. Čejka, *Catal. Rev.: Sci. Eng.*, 2014, **56**, 333–402.
2 T. F. Degnan, C. M. Smith and C. R. Venkat, *Appl. Catal., A*, 2001, **221**, 283–294.
3 J. Čejka and B. Wichterlová, *Catal. Rev.: Sci. Eng.*, 2002, **44**, 375–421.
4 W. Vermeiren and J.-P. Gilson, *Top. Catal.*, 2009, **52**, 1131–1161.
5 A. Corma, M. T. Portilla, C. Martínez, S. Valencia and F. J. Llopis, *Appl. Catal., A*, 2011, **393**, 257–268.
6 M. Moliner, J. González, M. T. Portilla, T. Willhammar, F. Rey, F. J. Llopis, X. Zou and A. Corma, *J. Am. Chem. Soc.*, 2011, **133**, 9497–9505.
7 A. Corma, C. Corell, F. Llopis, A. Martínez and J. Pérez-Pariente, *Appl. Catal., A*, 1994, **115**, 121–134.
8 A. Corma, A. Chica, J. M. Guil, F. J. Llopis, G. Mabilon, J. A. Perdigón-Melón and S. Valencia, *J. Catal.*, 2000, **189**, 382–394.
9 A. Corma, V. I. Costa-Vaya, M. J. Díaz-Cabañas and F. J. Llopis, *J. Catal.*, 2002, **207**, 46–56.
10 F. J. Llopis, G. Sastre and A. Corma, *J. Catal.*, 2004, **227**, 227–241.
11 A. Corma, F. J. Llopis, C. Martínez, G. Sastre and S. Valencia, *J. Catal.*, 2009, **268**, 9–17.

12 N. Zilkova, B. Gil, S. I. Zones, S. J. Hwang, M. Bejblova and J. Cejka, *Stud. Surf. Sci. Catal.*, 2008, **174B**, 1027–1032.
13 Z. Musilova-Pavlackova, M. Kubu, A. W. Burton, S. I. Zones, M. Bejblova and J. Cejka, *Catal. Lett.*, 2009, **131**, 393–400.
14 S. Al-Khattaf, Z. Musilová-Pavlačková, M. A. Ali and J. Čejka, *Top. Catal.*, 2009, **52**, 140–147.
15 C. Martinez and A. Corma, *Coord. Chem. Rev.*, 2011, **255**, 1558–1580.
16 J. S. Beck, A. B. Dandekar and T. F. Degnan, *Catal. Sci. Ser.*, 2002, **3**, 223–237.
17 T. F. Degnan, Jr., WO2000035836, Mobil Oil Corporation, 2000.
18 International Zeolite Asociation, http://www.iza-online.org/, (accessed 2011).
19 M. E. Leonowicz, J. A. Lawton, S. L. Lawton and M. K. Rubin, *Science*, 1994, **264**, 1910–1913.
20 C. Perego and P. Ingallina, *Catal. Today*, 2002, **73**, 3–22.
21 S. L. Lawton, M. E. Leonowicz, R. D. Partridge, P. Chu and M. K. Rubin, *Microporous Mesoporous Mater.*, 1998, **23**, 109–117.
22 G. G. Juttu and R. F. Lobo, *Microporous Mesoporous Mater.*, 2000, **40**, 9–23.
23 S. Laforge, D. Martin and M. Guisnet, *Microporous Mesoporous Mater.*, 2004, **67**, 235–244.
24 S. Laforge, D. Martin, J. L. Paillaud and M. Guisnet, *J. Catal.*, 2003, **220**, 92–103.
25 A. Corma, V. Martinez-Soria and E. Schnoeveld, *J. Catal.*, 2000, **192**, 163–173.
26 E. Dumitriu, D. Meloni, R. Monaci and V. Solinas, *C. R. Chim.*, 2005, **8**, 441–456.
27 W. J. Meng, B. H. Chen, Y. X. Li, C. Y. Li and G. Cao, *Shiyou Xuebao, Shiyou Jiagong*, 2003, **19**, 47–52.
28 G. Pop, R. Ganea, I. Tamas and C. Theodorescu, *Prog. Catal.*, 2003, **12**, 41–50.
29 H. O. Zhu, J. Wang and X. Q. Ren, *Nanjing Gongye Daxue Xuebao, Ziran Kexueban*, 2004, **26**, 24–26, 70.
30 Z. Zhu, Q. Chen, W. Zhu, D. Kong and C. Li, *Selections from the Presentations of the 3rd Asia-Pacific Congress*, 2004, vol. 93–95, pp. 321–325.
31 L. D. Fernandes, J. L. F. Monteiro, E. F. Sousa-Aguiar, A. Martinez and A. Corma, *J. Catal.*, 1998, **177**, 363–377.
32 M. Kollár, I. Kolev, M. R. Mihályi and V. Mavrodinova, *Appl. Catal., A*, 2011, **393**, 59–70.
33 M. T. Portilla, F. J. Llopis, C. Martínez, S. Valencia and A. Corma, *Appl. Catal., A*, 2011, **393**, 257–268.
34 M. R. Mihályi, I. Kolev, V. Mavrodinova, C. Minchev, M. Kollár and J. Valyon, *React. Kinet. Catal. Lett.*, 2007, **92**, 345–354.
35 S. H. Park and H. K. Rhee, *React. Kinet. Catal. Lett.*, 2003, **78**, 81–89.
36 A. van Miltenburg, J. Pawlesa, A. M. Bouzga, N. Žilková, J. Čejka and M. Stöcker, *Top. Catal.*, 2009, **52**, 1190–1202.
37 P. Wu, T. Komatsu and T. Yashima, *Microporous Mesoporous Mater.*, 1998, **22**, 343–356.
38 A. Corma, U. Diaz, V. Fornes, J. M. Guil, J. Martinez-Triguero and E. J. Creyghton, *J. Catal.*, 2000, **191**, 218–224.
39 A. Corma, V. Gonzalez-Alfaro and A. V. Orchilles, *Appl. Catal., A*, 1999, **187**, 245–254.
40 A. Corma and J. Martinez-Triguero, *J. Catal.*, 1997, **165**, 102–120.
41 K. Okumura, M. Hashimoto, T. Mimura and M. Niwa, *J. Catal.*, 2002, **206**, 23–28.
42 H.-K. Min, M. B. Park and S. B. Hong, *J. Catal.*, 2010, **271**, 186–194.
43 J. Hu, S. Wu, Z. Li, L. Peng, X. Fu, X. Wang, J. Guan and Q. Kan, *Appl. Organomet. Chem.*, 2015, **29**, 638–645.
44 M. T. Portilla, F. J. Llopis and C. Martínez, *Catal. Sci. Technol.*, 2015, **5**, 3806–3821.
45 X. Yin, N. Chu, J. Yang, J. Wang and Z. Li, *Catal. Commun.*, 2014, **43**, 218–222.
46 M. E. Domine, A. Corma Canos, V. Fornes Segui, U. Diaz Morales, J. L. Jorda Moret and F. Rey Garcia, WO2000034181, CSIC-UPV, 2000.
47 I. Rodriguez, M. J. Climent, S. Iborra, V. Fornes and A. Corma, *J. Catal.*, 2000, **192**, 441–447.
48 W. J. Roth, *Stud. Surf. Sci. Catal.*, 2007, **168**, 221–239.
49 W. J. Roth, C. T. Kresge, J. C. Vartuli, M. E. Leonowicz, A. S. Fung and S. B. McCullen, *Stud. Surf. Sci. Catal.*, 1995, **94**, 301–308.
50 A. Corma, V. Fornes, S. B. Pergher, T. Maesen and J. G. Buglass, *Nature*, 1998, **396**, 353–356.
51 A. Corma, V. Fornes, J. M. Guil, S. Pergher, T. L. M. Maesen and J. G. Buglass, *Microporous Mesoporous Mater.*, 2000, **38**, 301–309.
52 A. Corma, V. Fornes, J. Martinez-Triguero and S. B. Pergher, *J. Catal.*, 1999, **186**, 57–63.
53 P. Concepcion, C. Lopez, A. Martinez and V. F. Puntes, *J. Catal.*, 2004, **228**, 321–332.
54 A. Corma, H. Garcia and J. Miralles, *Microporous Mesoporous Mater.*, 2001, **43**, 161–169.
55 A. Corma, A. Martinez and V. Martinez-Soria, *J. Catal.*, 2001, **200**, 259–269.
56 W. J. Roth, P. Nachtigall, R. E. Morris and J. Čejka, *Chem. Rev.*, 2014, **114**, 4807–4837.
57 J. Wang, X. Tu, W. Hua, Y. Yue and Z. Gao, *Microporous Mesoporous Mater.*, 2011, **142**, 82–90.
58 J. Wang, F. Zhang, W. Hua, Y. Yue and Z. Gao, *Catal. Commun.*, 2012, **18**, 63–67.
59 U. Diaz and A. Corma, *Dalton Trans.*, 2014, **43**, 10292–10316.
60 C. A. Emeis, *J. Catal.*, 1993, **141**, 347–354.
61 A. Corma, V. Fornés, L. Forni, F. Márquez, J. Martínez-Triguero and D. Moscotti, *J. Catal.*, 1998, **179**, 451–458.
62 H. I. de Lasa, US5102628, Univ. Western Ontario, 1991.
63 S. Al-Khattaf and H. de Lasa, *Appl. Catal., A*, 2002, **226**, 139–153.
64 K. Toch, J. W. Thybaut, B. D. Vandegehuchte, C. S. L. Narasimhan, L. Domokos and G. B. Marin, *Appl. Catal., A*, 2012, **425–426**, 130–144.
65 S. Siffert, L. Gaillard and B. L. Su, *J. Mol. Catal. A: Chem.*, 2000, **153**, 267–279.
66 I. I. Ivanova, N. S. Nesterenko and C. Fernandez, *Catal. Today*, 2006, **113**, 115–125.
67 M. Moliner, J. González, M. T. Portilla, T. Willhammar, F. Rey, F. J. Llopis, X. Zou and A. Corma, *J. Am. Chem. Soc.*, 2011, **133**, 9497–9505.
68 Z. Musilová, N. Žilková, S. E. Park and J. Čejka, *Top. Catal.*, 2010, **53**, 1457–1469.

69 T. Odedairo, R. J. Balasamy and S. Al-Khattaf, *Ind. Eng. Chem. Res.*, 2011, **50**, 3169–3183.
70 N. Žilková, M. Bejblová, B. Gil, S. I. Zones, A. W. Burton, C. Y. Chen, Z. Musilová-Pavlačková, G. Košová and J. Čejka, *J. Catal.*, 2009, **266**, 79–91.
71 A. Corma and A. Martínez, in *Zeolites and Ordered Mesoporous Materials: Progress and Prospects*, ed. J. Čejka and H. V. Bekkum, 2005, p. 337.
72 I. I. Ivanova and A. Corma, *J. Phys. Chem. B*, 1997, **101**, 547–551.

